

Measurements of the Absolute Branching Fractions of $B^\pm \rightarrow K^\pm X_{c\bar{c}}$

Guy Wormser*

on behalf of the BABAR Collaboration

LAL, Univ. Paris-Sud, CNRS/IN2P3, Paris-Saclay University, Orsay, France

wormser@lal.in2p3.fr

A study of the two body decays $B^\pm \rightarrow X_{c\bar{c}} K^\pm$, where $X_{c\bar{c}}$ refers to one charmonium state, is reported by the *BABAR* experiment using a data sample of 424 fb^{-1} . The absolute determination of many branching fractions for these decays are significantly improved compared to previous *BABAR* measurements. Evidence is found at 3σ level for the decay $B^+ \rightarrow X(3872)K^+$. The absolute branching fraction $\text{BR}(B^+ \rightarrow X(3872)K^+) = (2.1 \pm 0.6(\text{stat}) \pm 0.3(\text{syst})) \cdot 10^{-4}$ is measured for the first time. From this, it follows that the branching fraction $\text{BR}(X(3872) \rightarrow J/\psi \pi^+ \pi^-)$ is equal to $(4.1 \pm 1.3)\%$, supporting the hypothesis of a molecular component for this resonance.

*European Physical Society Conference on High Energy Physics - EPS-HEP2019 -
10-17 July, 2019
Ghent, Belgium*

*Speaker.

In two-body B decays $B \rightarrow XK$, the X particle is predominantly a $c\bar{c}$ system with large available phase space. Many charmonium states are thus produced, with roughly equal rates when no strong selection rules apply [1]. They have been observed mostly using first an exclusive reconstruction of the charmonium state $X_{c\bar{c}}$ ($\eta_c, J/\psi, \chi_{c0}, \chi_{c1}, \eta_c(2S), \psi', \psi(3770)$), and the subsequent observation of the decay $B^\pm \rightarrow X_{c\bar{c}}K^\pm$ [2, 3]. The exotic charmonium state $X(3872)$, also known as $\chi_{c1}(3872)$, has also been reconstructed in this way [4, 5]. The determination of the absolute branching fraction $\text{BR}(B^+ \rightarrow X(3872)K^+)$ will then lead to the measurement of the absolute $\text{BR}(X(3872) \rightarrow J/\psi\pi^+\pi^-)$ which brings useful information regarding the complex nature of the $X(3872)$ particle. The original tetraquark model [6] predicted this branching fraction to be around 50%. A more refined tetraquark model [7] could accommodate a much smaller branching fraction, but requires the presence of another particle, $X(3876)$, which has not been observed. Various molecular models [8, 9] predict this BR below or equal to 10%. It is also pointed out [10] that a direct link can be made, using the deuterium analogy, between this BR and the production rate of the $X(3872)$ at hadron colliders. In addition, using the $X(3872)$ total width determination based on its line shape, or an upper limit on this quantity, information will be provided on the partial width $\Gamma(X(3872) \rightarrow J/\psi\pi^+\pi^-)$. A wide range of prediction exists for this partial width, from 1.3 MeV in the case of a pure charmonium state [11], to the 100 keV range for molecular models [8].

In this study, we adopt a technique, originally pioneered by BABAR [12], based on the measurement in the B rest frame of the kaon momentum spectrum, where each two-body decay can be identified by its characteristic monochromatic kaon spike. Taking advantage of the $Y(4S)$ decays to a B meson pair, the B center of mass frame is determined event by event by fully reconstructing the other B meson. The branching fractions for the two-body decays $B^\pm \rightarrow X_{c\bar{c}}K^\pm$ can thus be measured independently of any *a priori* knowledge of the $X_{c\bar{c}}$ decay properties.

For this analysis we use a data sample with an integrated luminosity of 424 fb^{-1} . The data have been collected with the BABAR detector at the PEP-II asymmetric energy storage ring, where 9 GeV electrons and 3.1 GeV positrons collide at a center of mass energy that corresponds to the mass of the $Y(4S)$ resonance. A detailed description of the BABAR detector can be found in [13]. Charged tracks are reconstructed with a 5 layer silicon vertex tracker (SVT) and a 40 layer drift chamber (DCH), located in a 1.5 T magnetic field generated by a superconducting solenoidal magnet. The energies of photons and electrons are measured with a CsI(Tl) electromagnetic calorimeter (EMC). Charged hadron identification is performed using ionization measurements in the SVT and DCH and using a ring imaging Čerenkov detector (DIRC). The instrumented flux return of the solenoid (IFR) is used to identify muons.

The analysis method is a recoil technique similar to that presented in [12]. The complete exclusive reconstruction of one of the two B mesons produced in the event provides access to the rest frame of the other B meson in which signal events are two-body B^\pm decays to $K^\pm X$. For such decays, the kaon momentum in the B center-of-mass frame, p_k exhibits a peak for each X particle from which its mass, m_X is equal to $\sqrt{m_B^2 m_K^2 - 2E_K m_B}$, where m_B and m_K are the masses of the B and K mesons and E_K is the kaon energy in the B center of mass. The p_k spectrum will contain, in addition to the series of signal peaks, a continuum due to kaons coming from non 2-body decays or from decays of charmed mesons. We determine the number of each observed charmonium resonance $X_{c\bar{c}}$ from a fit to the K momentum distribution.

The first step in event selection requires the full reconstruction of a tagging B^\pm meson in the event, (B -tag). B -tag mesons are reconstructed in $B \rightarrow SY$ decays, where the seed S is a fully reconstructed D^0 , D^\pm , D_s^\pm , or J/ψ meson, and Y represents a hadronic state, combining π^\pm , K^\pm , π^0 , and K_S^0 hadrons [14]. For each one of these modes, the purity (defined as $S/(S+B)$, where S is the number of signal events and B the number of background events) have been determined. A minimum purity of 0.08 is required. The number of B candidates is determined with a fit to the distribution of the B -energy-substituted mass, $m_{ES} = \sqrt{E_{CM}^2/4 - p_B^2}$, where E_{CM} is the B total center of mass energy, determined from the beam parameters, and p_B is the measured momentum of the reconstructed B in this $\Upsilon(4S)$ rest frame. The fit function is the sum of a Crystal Ball function describing the signal [15] and an Argus function for the background [16]. The fit is displayed in Fig. 1. The number of fully reconstructed B^\pm decays found by the fit is $1,67 \cdot 10^6$

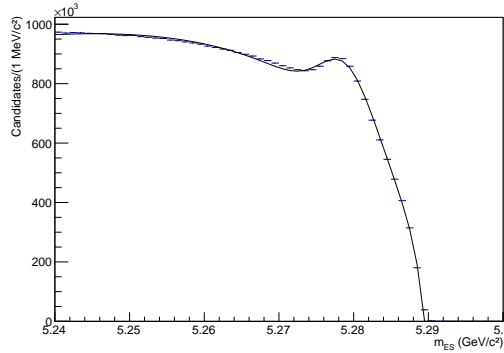


Figure 1: The m_{ES} distribution of all the exclusively reconstructed B^\pm . A better agreement between the data and the fit function would have required a separate fit per running period, which is not necessary for this analysis.

$\pm 4, 2 \cdot 10^3$ (stat) $\pm 6, 4 \cdot 10^4$ (syst) B^\pm . The systematic uncertainty is dominated by the background shape near the kinematical end-point.

If more than one B candidate is found in a given event, all candidates are retained. This is an important difference compared to Ref. [12] and also the subsequent BELLE analysis [17], where only one candidate per event was retained. The reason for this change is two-fold; increase the efficiency and to decouple as much as possible the signal and tag sides in B^+B^- events. B candidates coming from the full or quasi-full reconstruction of a signal decay channel should not be considered as the only tag as this would lead to discard another genuine tag and a signal loss. The mean number of B -tag candidates per event is 1.85. The maximum efficiency improvement is a factor 3 for the $X(3872)$ because of its decays to D mesons that create B -tag seeds.

The selection cuts used in the analysis are thus very few : each B -tag candidate should have $m_{ES} > 5.275$ GeV/c and be accompanied by an opposite-sign kaon candidate, passing the tight particle identification cut. The pion contamination in this kaon sample is below 2%. A first neural network (NN) is then used to suppress the continuum background. The inputs to the NN are 7 variables related to the reconstructed B characteristics, to its production kinematics, to the topology of the full event and to the angular correlation between the reconstructed B and the rest of the event. The NN selection has an 80% efficiency for generic B^+B^- events and a factor 10 rejection against

non- B background events coming from u, d, s , or c quark-antiquark pairs.

A second NN is used to reject secondary kaons produced in B -daughters D mesons decays. This is a large background which increases rapidly with decreasing kaon momenta. In the B rest frame, the secondary kaons are embedded in the D decay products, which, given the boost of the D meson and its mass, are bounded in a cone and form a wide jet, whereas primary kaons (those forming the signal of this analysis) recoil against a massive (3 to 4 GeV/c²) state tend to be more isolated, with the rest of the B decay products being more spherical. The input variables to this NN take advantage of these characteristics [12]. These two NN are then combined in a single neural net, called SuperNN, to optimize further the signal to noise. Because of the non negligible (but slow) variation of the event topology with the mass of the charmonium particle, the SuperNN is trained separately in the J/ψ and η_c signal peaks region, and in the ψ' and $\eta_c(2S)$ region, with kaon background taken from simulation in the ranges 1.6 to 1.9 GeV and 1.2 to 1.5 GeV regions, respectively. The SuperNN performance corresponds to a 72% signal efficiency at the $X(3872)$ peak and a rejection background factor varying between 3 in the $X(3872)$ and ψ' region and 4.5 in the J/ψ region.

The procedure followed to extract the results is in two steps: firstly determination of the background shape from an interpolation of data points where no signal is present, secondly, a fit to background subtracted data. The shape of the kaon momentum for background kaons is determined from an interpolation through data points from regions where no signal is expected, below 1.1 GeV/c and above 1.9 GeV/c. Using only these two regions leads, however, to large uncertainty in the PDF parameters. It is therefore necessary to add no-signal data points in the two regions 1.34-1.36 GeV/c, and 1.53-1.57 GeV/c, where there is no peak, as indicated on Fig. 2.

Fig. 2 also shows, at the bottom, the fit to the signal K^\pm momentum spectrum for all charmonia peaks in the simulation. A good description is obtained when using, for each peak, a narrow Gaussian, whose width depends on momentum varying from 13 MeV/c for the J/ψ to 9 MeV/c for the ψ' , and an asymmetric Gaussian, 100 MeV/c wide on the left and 60 MeV/c wide on the right. A similar fit is performed for the $X(3872)$ with a dedicated Monte Carlo sample and is shown in Fig. 3. The narrow width is measured to be 7 MeV/c and the wide Gaussian tails are 47 MeV/c on each side. The wide Gaussian is associated with candidates where the B -tag has a reconstructed m_{ES} in the signal region but is not build with the exact set of the B decay products and therefore provides an incorrect boost. The relative importance of the wide Gaussian term is therefore proportional to the background under the B mass peak. The level of this background depends of the signal-side final state, particularly on whether the charmonium state decays to a final state containing open-charm mesons, such as the $\psi(3770)$ or the $X(3872)$. This effect is beneficial since it induces a higher efficiency for the $X(3872)$: the MC efficiency is found to be $(0.25 \pm 0.07)\%$ for $J/\psi K^\pm$ events and $(0.77 \pm 0.02)\%$ for $X(3872)K^\pm$ events. It however gives rise to systematic uncertainties in the signal shape, due to the limited knowledge of the decay channels of the particle under study.

When using the intermediate points to interpolate the background, one has to take into account that the tails from the J/ψ and $\eta_c(2S)$ peaks extend in these intermediate regions. They are subtracted using the Monte Carlo where the known branching fractions for the corresponding resonances [18] are included. The relative systematic uncertainty of the signal yields resulting from this procedure, in case of a difference between true and predicted contributions of the tails

of the charmonia particles in these regions, are found to be 4%. The fit function is a product of Tchebyshev polynomials of order 5 and an exponential function.

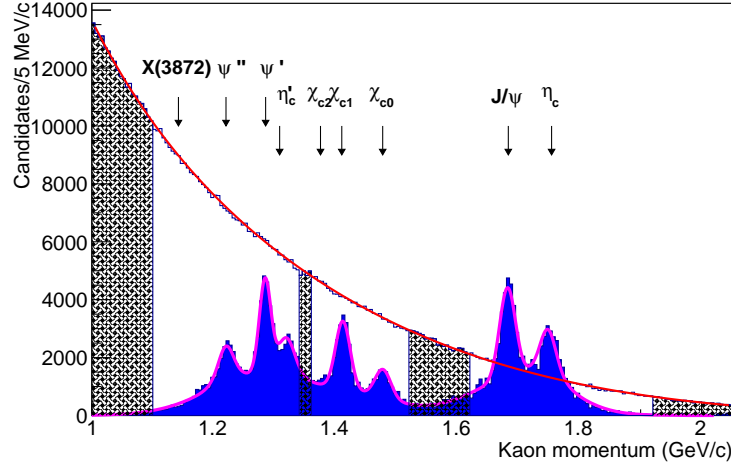


Figure 2: K^\pm momentum spectrum for simulated events where no-signal K^\pm are present. The hatched areas correspond to the no-signal zones used to fit the polynomial background. The filled blue histogram is the signal-only K^\pm momentum spectrum in simulated events. The purple line represents the fit to this distribution.

The small residual pulls are observed in the simulation between the p_K distribution and the fit function. These defects in background shape do not affect the visibility of narrow peaks, such as that of the $X(3872)$, since the expected width of 7 MeV/c is much smaller than the 50 MeV/c typical width of the local variations. In particular, the observed pulls in the 1.1 to 1.2 GeV/c region are corrected for, and the resulting uncertainty is taken into account.

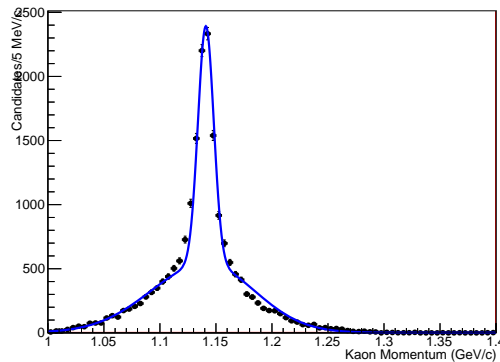


Figure 3: Fit to the signal-only K^\pm momentum spectrum in $X(3872)$ simulated events.

The data kaon momentum spectrum between 1.5 and 2 GeV/c is expected to exhibit two peaks, one at $p_k = 1.684$ GeV/c corresponding to the J/ψ and the second at $p_k = 1.754$ GeV/c for the η_c meson. The SuperNN is trained in the J/ψ - η_c region. The selection requires a value of the superNN output >0.85 and a B purity larger than 0.08. The background-subtracted spectrum is

fitted with two signal functions determined above, the only free parameters being the charmonia yields. The fit results are displayed in Fig. 4, with the following yields: $N_{J/\psi} = 2364 \pm 189$ and $N_{\eta_c} = 2259 \pm 188$. The statistical precision obtained on the J/ψ and η_c yields is 8%, a factor 2 improvement compared to [12].

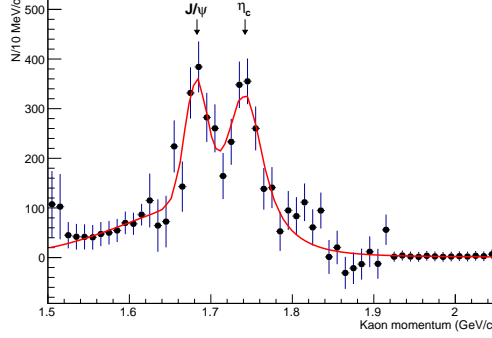


Figure 4: Background-subtracted kaon momentum spectrum in the J/ψ - η_c region.

The branching fractions $\text{BF}(B^\pm \rightarrow K^\pm \eta_c)$ is computed using the world average $\text{BF}(B^\pm \rightarrow K^\pm J/\psi)$ [18] and the ratio of the yields quoted above, to obtain:

$\text{BF}(B^\pm \rightarrow K^\pm \eta_c) = (0.96 \pm 0.12(\text{stat}) \pm 0.06(\text{syst}) \pm 0.03(\text{“ref”})) \cdot 10^{-3}$, where the systematic uncertainty is detailed in Table 1, and “ref” refers to the uncertainty of the branching fraction $\text{BF}(B^\pm \rightarrow K^\pm J/\psi)$ [18]. This result agrees with the present world average for this branching fraction $(1.09 \pm 0.09) \cdot 10^{-3}$ [18]. As a cross-check, the $\text{BF}(B^\pm \rightarrow K^\pm J/\psi)$ is also extracted from the ratio of observed J/ψ events obtained in data and simulation: $\text{BF}(B^\pm \rightarrow K^\pm J/\psi) = (1.09 \pm 0.9((\text{stat}) \pm 0.6(\text{syst})) \cdot 10^{-3}$, in good agreement with present world average.

For the high mass region, the SuperNN is trained using the ψ' domain. The selection requires the SuperNN- ψ' output value > 0.6 and the B purity larger than 0.10. The background shape is determined using a fit to the signal free-region after correction for the small signal residual in that region estimated from the MC simulation. The kaon momentum spectrum before background subtraction is displayed in Fig. 5.

The fitted signal is the sum of 9 signal-peak functions corresponding to the nine particles: $X(3872)$, $\psi(3770)$, ψ' , $\eta_c(2S)$, χ_{c2} , χ_{c1} and χ_{c0} , J/ψ , and η_c . The peak locations are taken from [18] and the widths are obtained from fits to MC signal samples and account for both detector resolution and the natural width of each resonance. The peak labelled χ_{c1} refers to both χ_{c1} and h_c since h_c and χ_{c1} cannot be distinguished from each other in this analysis. A binned maximum likelihood fit is used for the fit to the data, with the nine charmonia yields as free parameters. The results are shown in Fig. 6 in the range 1.-2.05 GeV/c. Table 2 contains the fit results. Signal peaks are visible for η_c , J/ψ , χ_{c1} , ψ' , and for the $X(3872)$ state. A separate fit in which the $X(3872)$ signal is forced to 0 has a χ^2 larger than that of the nominal fit by 11.1 units but, by 9.0 only when taking into account the uncertainty in the background shape in the region 1.1 to 1.2 GeV/c. Thus, there is evidence of the decay $B^\pm \rightarrow X(3872)$, detected for the first time using this recoil technique with a significance of 3σ .

The systematic uncertainties associated with this analysis method mainly stem from the im-

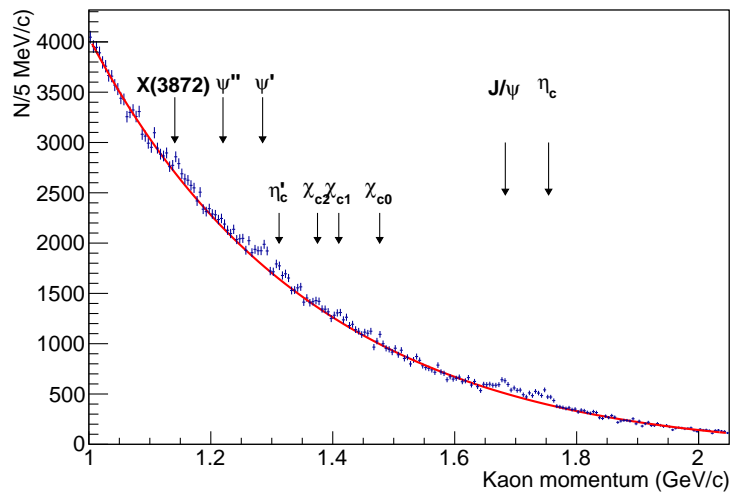


Figure 5: Kaon momentum spectrum after final selection cuts and before background subtraction. The red line is the interpolated function describing background shape. The arrows indicate the values at which the signal for each resonance is expected.

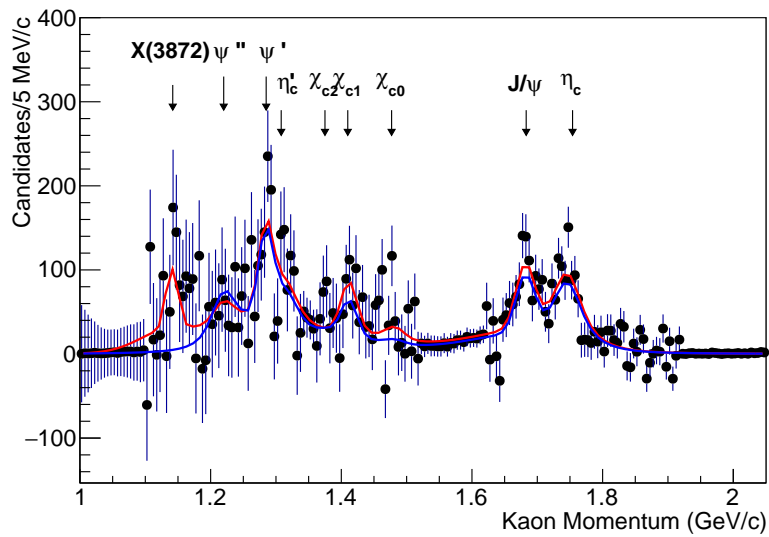


Figure 6: Kaon momentum spectrum between 1. and 2.05 GeV/c. The fit function include signal peaks for 9 particles, indicated by the arrows.

perfect description of the data by the simulation. They are similar for all the resonances studied and are computed in detail for two of them, η_c and $X(3872)$:

- *Peak position.* A potential deviation from the known peak position can induce an uncertainty in the number of events from the fit integral. The effect is found to be 1%.
- *Signal shape.* Four parameters are used to describe the signal shape: the main narrow width of the signal peak, the widths of the left and right Gaussian tails, and the relative fraction of the narrow Gaussian over the total. The systematic uncertainties regarding the signal shape are computed by taking the one standard-deviation interval extracted from the signal-only fit performed to the simulation sample. When the peak position has a non-negligible natural width, such as in the case of the η_c , the uncertainty coming from the limited knowledge of the width is also taken into account.
- *Background subtraction.* Systematic uncertainties are related to the arbitrary mathematical form of the interpolation function. The uncertainty of the background fit is propagated including correlations, into the signal statistical uncertainty and is therefore not accounted as a systematic uncertainty. However, the uncertainty due to the correction due to the signal subtraction in the region 1.1 to 1.2 GeV/c implies sizeable corrections for the $X(3872)$ yield. This uncertainty is determined by taking the effect on the $X(3872)$ yield introduced by a 1-sigma deviation of the correction function, and is determined to be 13%.
- *Efficiency determination.* The associated uncertainties relate to the kaon reconstruction and PID-selection efficiencies, and to the SuperNN-based selection. It is important to note that these uncertainties cancel to a very good approximation in the ratio of the branching fractions of all resonances to the J/ψ .

Finally, another source of systematic uncertainty, specific to the $X(3872)$, is caused by the uncertainty in its decay model. The signal shape, as mentioned above, is not the same for DD and $J/\psi X$ decays and this effect induces a small change in the signal yield in the fit. Varying the ratio between these two types of decays in the present allowed range leads to a 5% additional systematic uncertainty. Table 1 summarizes the various systematic uncertainty sources, and Table 2 summarizes the branching fractions results for all resonances.

The observed number of $X(3872)$ events is converted into an absolute branching fraction using the number of observed J/ψ events, its absolute branching fraction, and the relative efficiency ratio and is found to be : $BR(B^+ \rightarrow X(3872)K^+) = (2.1 \pm 0.6)((\text{stat})) \pm 0.3((\text{syst})) \pm 0.1((\text{ref}))) \times 10^{-4}$, where “ref” refers to the uncertainty in the reference $BR(B^+ \rightarrow J/\psi K^+)$ [18]. This translates, using the measured rate of $BR(B^+ \rightarrow X(3872)K^+) \times BR(X(3872) \rightarrow J/\psi \pi^+ \pi^-)$ of $(8.6 \pm 0.8) \times 10^{-6}$, into $BR(X(3872) \rightarrow J/\psi \pi^+ \pi^-) = (4.1 \pm 1.3)\%$. From this, an upper limit of the $\Gamma(X(3872) \rightarrow J/\psi \pi^+ \pi^-)$ partial width can be set in the 100 keV range, using 3 MeV as an upper limit for the $X(3872)$ total width, as measured in its DD decay channel [19, 20]. Our measurement therefore suggests that the $X(3872)$ has a significant molecular component.

In summary, the update of our first analysis [12] with the full *BABAR* statistics is reported. Two new features are introduced: the inclusion of all B candidates has led to an increase of efficiency

Uncertainty source	η_c (%)	$X(3872)$ (%)
K identification	1	5
Decay model	-	5
Efficiency	0	5
p_K spectrum: peak position	2	2
p_K spectrum: signal narrow width	1	1
p_K spectrum: signal wide width	5	5
p_K spectrum: narrow width fraction	2	2
p_K spectrum: background shape	-	13
Decay width	1	-
Correction in signal-free regions	-	4
Total	6	16.3

Table 1: Summary of relative systematic uncertainties (in %) for the η_c and $X(3872)$ resonances branching fraction measurements, relative to $\text{BR}(B^\pm \rightarrow J/\psi K^\pm)$.

Particle	Yield	BF(10^{-4})
J/ψ	2364 ± 189	10.1 ± 0.29 (Ref from [18])
η_c	2259 ± 188	$9.6 \pm 1.2(\text{stat}) \pm 0.6(\text{sys})$
χ_{c0}	287 ± 181	$2.0 \pm 1.3(\text{sat}) \pm 0.3(\text{sys})$
χ_{c1}	1035 ± 193	$4.0 \pm 0.8(\text{stat}) \pm 0.6(\text{sys})$
χ_{c2}	200 ± 164	< 2.0
$\eta_c(2S)$	527 ± 271	$3.4 \pm 1.7(\text{stat}) \pm 0.5(\text{sys})$
ψ'	1278 ± 285	$4.6 \pm 1(\text{stat}) \pm 0.7(\text{sys})$
$\psi(3770)$	497 ± 308	$3.2 \pm 2.0(\text{stat}) \pm 0.5(\text{syst})$
$X(3872)$	992 ± 285	$2.1 \pm 0.6(\text{stat}) \pm 0.3(\text{syst})$

Table 2: Results from fits to the K momentum spectrum. BF stands for the branching fraction of the decay $B^\pm \rightarrow X_{c\bar{c}} K^\pm$. An additional relative 3% uncertainty must be added to all the results, reflecting the present knowledge of the reference $\text{BR}(B^+ \rightarrow J/\psi K^+)$.

and a better separation between signal and tag-sides of an event; moreover, the fit of the polynomial background in regions where no signal is present has reduced the statistical and systematic uncertainties related to the background subtraction. This has led to the following results:

$$\text{BR}(B^+ \rightarrow \eta_c K^+) = (0.96 \pm 0.12(\text{stat}) \pm 0.06(\text{syst}) \pm 0.03(\text{ref})) \cdot 10^{-3},$$

$$\text{BR}(B^+ \rightarrow X(3872) K^+) = (2.1 \pm 0.6(\text{stat}) \pm 0.3(\text{syst}) \pm 0.1(\text{ref})) \cdot 10^{-4},$$

$$\text{BR}(X(3872) \rightarrow J/\psi \pi^+ \pi^-) = (4.1 \pm 1.3)\%,$$

using the measured rate of $X(3872)$ produced in B^+ decays and decaying into $J/\psi \pi^+ \pi^-$ ([18]). This result will certainly contribute to the determination of the complex nature of the $X(3872)$ particle.

We are grateful for the extraordinary contributions of our PEP-II colleagues in achieving the excellent luminosity and machine conditions that have made this work possible. The success of this project also relies critically on the expertise and dedication of the computing organizations that support *BABAR*. The collaborating institutions wish to thank SLAC for its support and the kind hospitality extended to them. This work is supported by the US Department of Energy and National Science Foundation, the Natural Sciences and Engineering Research Council (Canada), Institute of High Energy Physics (China), the Commissariat à l’Energie Atomique and Institut National de Physique Nucléaire et de Physique des Particules (France), the Bundesministerium für Bildung und Forschung and Deutsche Forschungsgemeinschaft (Germany), the Istituto Nazionale di Fisica Nucleare (Italy), the Foundation for Fundamental Research on Matter (The Netherlands), the Research Council of Norway, the Ministry of Science and Technology of the Russian Federation, and the Particle Physics and Astronomy Research Council (United Kingdom). Individuals have received support from CONACyT (Mexico), the A. P. Sloan Foundation, the Research Corporation, and the Alexander von Humboldt Foundation.

References

- [1] C. Quigg, FERMILAB-Conf-04/033-T, and hep-ph/0403187, and references therein.
- [2] B. Aubert et al., *BABAR* Collaboration, Phys.Rev.D **67**, 032002 (2003).
- [3] S.-K.Choi, S.L.Olsen, et al., Belle Collaboration, Phys. Rev. Lett. **89**, 102001 (2002).
- [4] Choi, S.K. et al., Belle Collaboration, Phys.Rev. D **84**, 052004 (2011).
- [5] B.Aubert et al., *BABAR* Collaboration, Phys. Rev. D **77**, 111101 (2008)
- [6] L. Maiani, et al., Phys. Rev. D **71**, 014028 (2005).
- [7] L. Maiani, et al., Phys. Rev. Lett. **99**, 182003 (2007).
- [8] E. Braaten et al., Phys. Rev. D **72**, 054022 (2005).
- [9] T.Barnes,S. Godfrey, Phys. Rev. D **69**, 054008 (2004).
- [10] P.G.Ortega, E.R. Arriola, hep-ph1907-01441.
- [11] E. Swanson, Phys. Lett. B, **588**, 189-195 (2004).
- [12] B.Aubert et al., *BABAR* Collaboration, Phys. Rev. Lett. **96**, 052002 (2006).
- [13] B. Aubert, et al. *BABAR* Collaboration, Nucl. Instr. Meth. A 479, 1 (2002). and B. Aubert et al., *BABAR* Collaboration, Nucl.Instrum.Meth. A729 (2013) 615-701.
- [14] B.Aubert et al., *BABAR* Collaboration, Phys. Rev. Lett. **109**, 101802 (2012).
- [15] T.Skwarnicki et al., DESY-F31-86-02.
- [16] H.Albrecht et al., (ARGUS Collaboration), Phys. Lett. B318,397 (1993).
- [17] Y. Kato et al. , BELLE Collaboration, Phys. Rev. D**97** 012005 (2018).
- [18] M. Tanabashi et al. (Particle Data Group), Phys. Rev. D 98, 030001 (2018) and 2019 update.
- [19] B. Aubert et al., *BABAR* Collaboration, Phys. Rev. D**77** 011102 (2008).
- [20] T. Aushev et al., BELLE Collaboration, Phys. Rev. D**81** 031103 (2010).